Theoretical Analysis and Reaction Mechanisms for Experimental Results of Hydrogen-Nickel Systems

Yeong E. Kim[1] and John Hadjichristos [2]

[1]Department of Physics, Purdue University, West Lafayette, Indiana 47907, USA, yekim@purdue.edu
[2]Defkalion Green Technologies Corporation, 1140 Homer Street, Suite 250, Vancouver BC V682X6, Canada

Abstract—**Experimental results for anomalous heat effect and super magnetic field observed for hydrogen-Nickel systems are described. Theoretical analysis and reaction mechanisms are presented using theory of Boson cluster state nuclear fusion (BCSNF) based on the optical theorem formulation. Observed excess heat generation and anomalously large magnetic field are explained by theoretical descriptions based on nano-scale explosions ("Bosenova") and proton supper currents.**

Index Terms—**Hydrogen fusion in metals, Boson cluster state nuclear fusion, excess heat generation, anomalous super magnetic field.**

1. Introduction

Recently, the experimental results of excess heat generation with hydrogen-Nickel systems have been reported [1]. Over the past twenty four years, there have been many publications reporting experimental observations of excess heat generation and anomalous nuclear reactions occurring in metals at ultra-low energies, now known as the Fleischmann-Pons effect [2, 3] which include both electrolysis and gas loading experiments [3-5] and also include experiments involving deuterium-metals [2-5] and hydrogen-metals [1,6-9]. Theoretical explanations of the Fleischmann-Pons effect [2,3] and the low energy nuclear phenomena [2-5] have been described based on the theory of Bose-Einstein condensation nuclear fusion (BECNF) or theory of Boson cluster state nuclear fusion (BCSNF), occurring in micro/nano-scale traps/metal particles [10-24].

In this paper, we describe the results of the earlier experimental work [1] as well as the more recent results of experiments with hydrogen-Nickel systems, including the observation of generation of anomalously large magnetic field ("super magnetic field"). After reporting the experimental results, we describe theoretical analysis and reaction mechanisms for the observed experimental results of hydrogen-Nickel systems based on the BCSNF theory [10-24].

2. Experimental Techniques and Procedures

2.1. Experimental device/fuels/reaction cells

The experimental results reported in this paper are based on Hyperion R5 lab reactors, for which the reactor geometries are shown in Fig. 1 below (some details omitted).
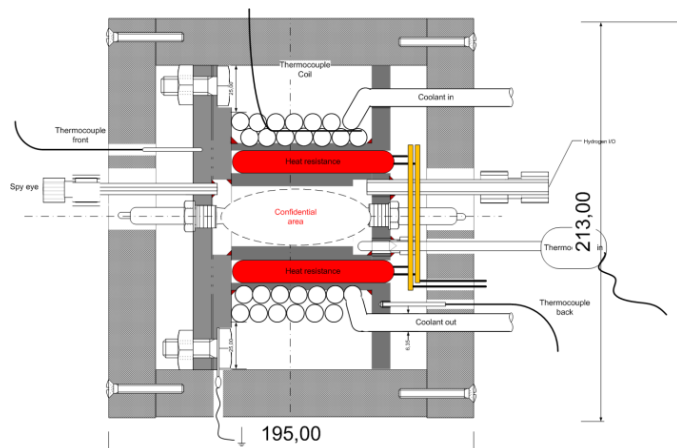

Fig.1   Hyperion Lab Prototype architecture (in mm)

Reactor's chamber, constructed with SS316, was hermitically sealed following its degassing and H_2 pump at 1.2bars. The Hyperion reactor contains a reactor core of Ni metal foam with many empty cells with average diameter of ~200 microns (μm). Each core is filled with Ni powders of ~ 5 microns (μm). Ni grains had been modified following a proprietary method as described in [1]. The core is supported with a ceramic structure and mu metal layers.

2.2. Triggering method

The triggering of the reactions is performed by a HV DC pulsed discharge between W and TZM electrodes (10-24kV, 60-110mA) at a kHz pulse range. This periodic triggering follows the initial pre-heating of the active material at temperature higher than 179^oC, using electric heat resistors embedded in the reactor's structure as in shown in Fig. 1. Both energy input and electric power sources were controlled and modulated through VARIACs.

2.3. Experimental measurement techniques

All input power and signals from the attached thermocouples, gamma detectors and the flow meter of the water which cools the reactor through the Cu coil rounding it, were monitored in real time per sec through a NI Labview/PCX data acquisition board. The detailed configuration of the data acquisition, the calorimeter setup and the calibration check of all measuring devises is presented in details in [25].

Overall cross checking of the system's performance was performed with a control test using the same system, operating with identical input and coolant flow parameters, except replacing only the H_2 gas with Ar gas at the same initial pump-in pressure.

For specific parameters measurements, such as the excited levels of H_2 or hydrogen atom excitation to their Rydberg states or the magnetic field emissions, a modified version of the Hyperion R5 reactor, as described in the section 2.1, was used. In such measurements, photoemissions from Rydberg state (5<n<85) species, such as H, were detected and measured using Raman type spectroscopy through a "spy-eye" attached in the reactor, while mu metals were removed.

For the magnetic fields measurements, mu metals were removed. Three GMO8 Hirst Magnetic Instruments Gauss meters were used, data logging per sec DC or DC peaks using an synchronized clock with the NI/PCX data acquisition system's clock. Each Gauss meter was attached to a TP002 traverse Hall probe, vertically aligned to the magnetic field lines created inside the reactor by the HV currents. The TP002 probes were held at the top, front and back from the center of the reactor chamber at positions with distances 18cm from the axes defined by the spark plugs (dotted lines on Fig. 1). In Fig. 1, the first one at the top on the page, the second one at the back into the page, the third one at the front out of the page, all from the center of the reaction chamber. Measured magnetic field strengths were similar, but not identical, at these three different locations.

3. Experimental Results

3.1. Excess energy measurements

Following the protocol defined in [25] in a series of tests conducted in Defkalion GT labs at Vancouver, BC, Canada (14th to 16th of May 2013), the following data and performance is reported for the active test using H_2.
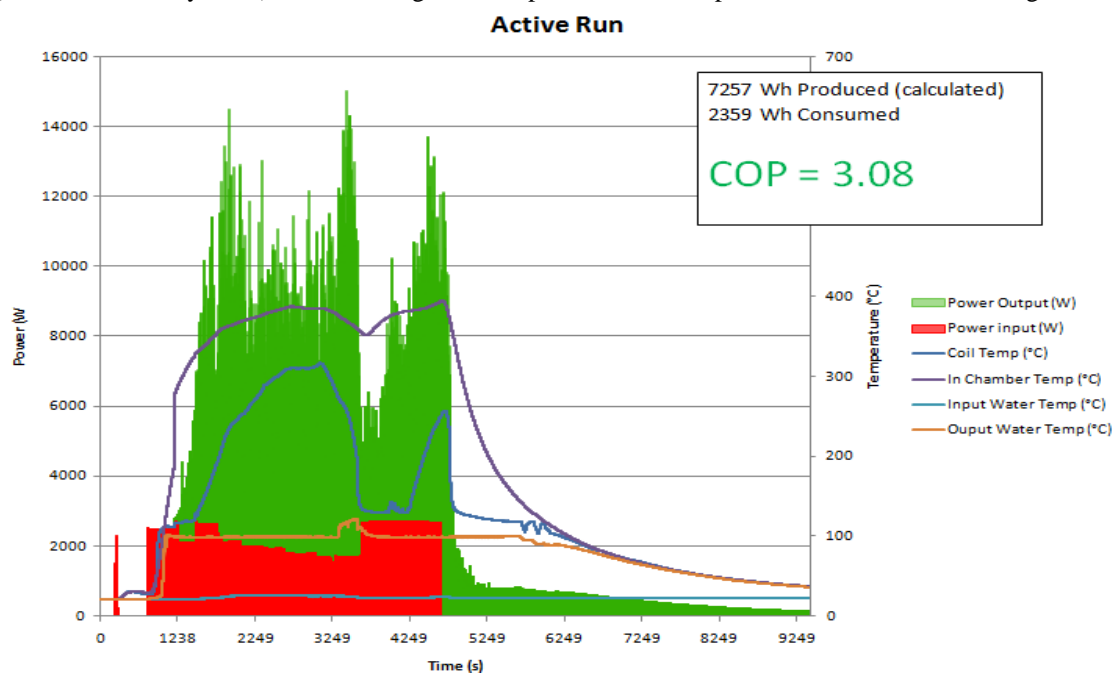

Fig. 2. Calorimeter and thermal signals (active test)

Using the same color indicators, the equivalent control run measurements, using Ar instead of H_2, were presented in Fig. 3:
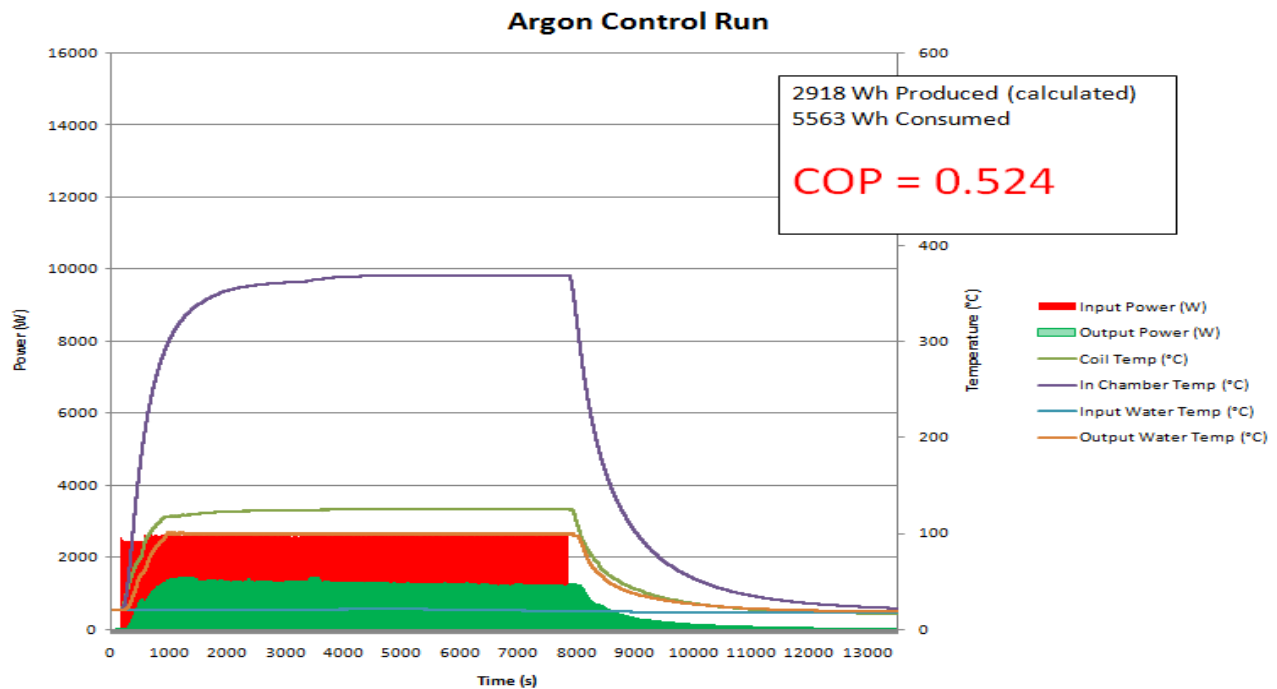

Fig. 3   Calorimeter and thermal signals (Ar control test)

For the power output calculation, it was assumed that water was cooling the reactor at liquid phase, even though its temperature within the coil surrounding the reactor was logged at temperatures greater than 230°C.

Such tests indicate the production of excess heat energy far above any known chemical reaction.

3.2 Radiation measurements

As shown in Fig. 4, no gamma rays outside the energy range of 50 keV–300 keV have been observed from the experiments with the Hyperion R-5 reactor (data are from iso-parabolic calorimeter experiment carried out on May 6, 2013).

3.3. Magnetic field measurements

After each triggering duty cycle (the triggering sequences producing excess heat), the magnetic fields at ~18 cm from the reactor at all three locations rose from ~0.6 Tesla to ~1.6 Tesla (DC peak) during each reaction period. Such anomalous peak signals were maintained for approximately 3-4 sec after the HV currents were cut off. This indicates that interactions/reactions within the reactor are producing very strong electric fields E (and currents I plus nano-plasma) between the Ni grain nano-antennas, as suggested by Ostrikov et al. [26], and very strong magnetic fields B, possibly enhanced by gallery whisper effects due to reactor's internal structure and geometry. Such strong magnetic fields are used within Hyperion reactor's architecture to stabilize the plasma generated by the HV discharges in non-vacuum conditions.

A new series of protocols and tests is expected to investigate the possible role of metal surface plasmons on the active Ni crystals lattice, as described by Durach et al. [27], for such "anomalous" magnetic field emissions and their role in the reactions, as predicted in section 7.

3.4. Even-isotope effect measurements

It was reported by Hadjichristos et al. [1] that the Hyperion reactor with each of even isotopes of Ni (^{58}Ni, ^{60}Ni, ^{62}Ni, and ^{64}Ni) produced excess heat as described in sub-section 3.1, while the odd Ni isotope ^{61}Ni did not, even though all single isotope crystals were treated using the same preparation and triggering protocols.

This type of experiments will be repeated, using the real time mass spectrometer described in [28].
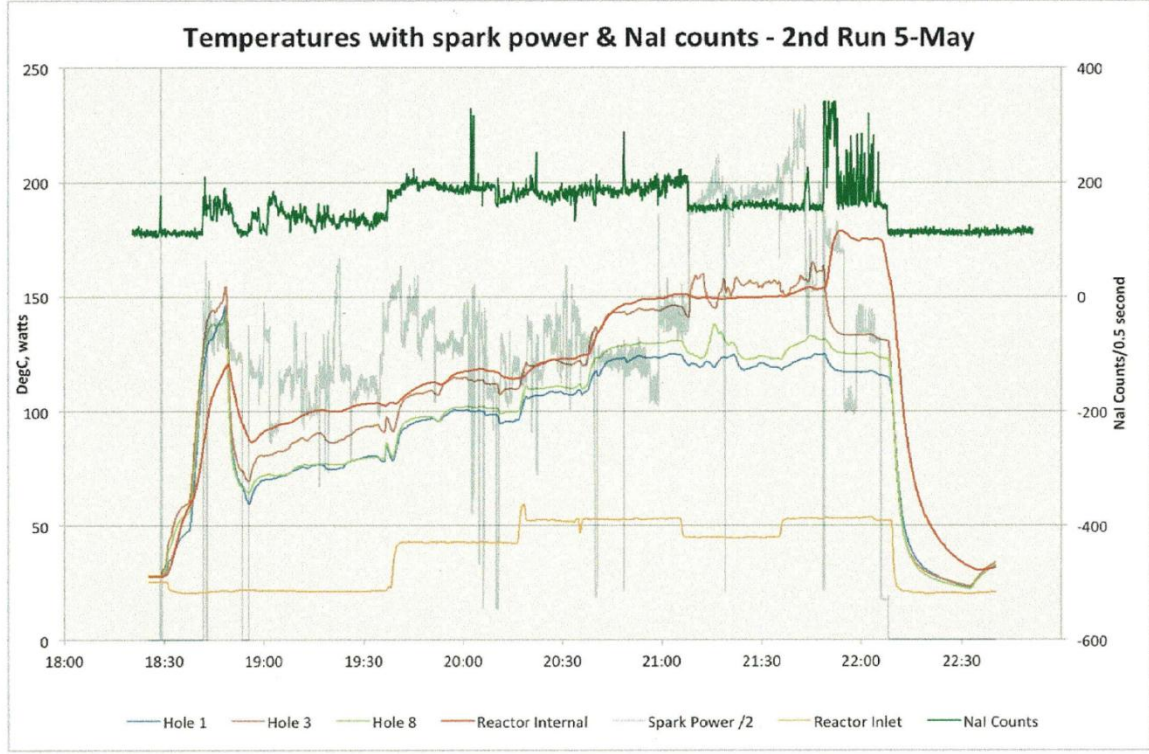
NaI counts with thermal data

Fig. 4   NaI counts versus thermal signals

4. Conventional Theory of Low-Energy Nuclear Reactions

The BECNF theory or theory of Boson cluster state nuclear fusion (BCSNF) is based on a single basic assumption capable of explaining the observed phenomena; deuterons in metals undergo Boson cluster state (BCS) formation or Bose-Einstein condensation (BEC).

4.1. Optical theorem formulation of reaction rates (OPT-RRs)

In this section, we describe theoretical derivation of the reaction rates for the BCSNF theory based on the optical theorem formulation of the low-energy nuclear reactions.

Based on the optical theorem, the following optical theorem formula was derived in reference [10]

$$\operatorname{Im} f_t^{n(el)} \approx \frac{k}{4\pi} \sigma_t^r \tag{1}$$

where $f_t^{n(el)}$ and σ_t^r are the l-th partial wave nuclear elastic scattering amplitude and reaction cross-section, respectively. The above formula is rigorous at low energies.

The elastic scattering amplitude can be written in terms of t-matrix as

$$f_t^{n(el)} = -\frac{2\mu}{\hbar^2 k^2} < \psi_t^c \left| t_t \right| \psi_t^c > \tag{2}$$

where ψ_l^c is the Coulomb wave function for scattering between two charged particles. From Eqs. (1) and (2), we obtain the optical theorem formula for the dominant s-wave state as:

$$\frac{k}{4\pi} \sigma^r = -\frac{2\mu}{\hbar^2 k^2} < \psi_0^c \left| \operatorname{Im} t_0 \right| \psi_0^c > \tag{3}$$

with

$$\sigma^r = \frac{S}{E} e^{-2\pi\eta} \quad and \quad \operatorname{Im} t = -\frac{S r_B}{4\pi^2} \delta(\vec{r}) \tag{4}$$

where
$$r_B = \frac{\hbar}{2\mu e^2} \quad with \quad \mu = \frac{m_i m_j}{m_i + m_j}$$

The reaction rate is given by

$$R = v\sigma^r = -<\psi^c|\mathrm{Im}V|\psi^c> \tag{5}$$

with Fermi potential

$$\mathrm{Im}V = -A\delta(\vec{r}_{ij}), \qquad A = \left(\frac{2}{\hbar}\right)\frac{Sr_B}{\pi}$$

where S is called astrophysical S-factor and related to the nuclear force strength. The delta-function represents the short-range nature of the nuclear force.

4.2. Generalization to low-energy nuclear phenomena in metals

The above result given by Eq. (5) can be generalized to D+D fusion reactions in metals to obtain

$$R_t = -\frac{2}{\hbar}\frac{\Sigma_{i<j}<\Psi|\mathrm{Im}V_{ij}^F|\Psi>}{<\Psi|\Psi>} \tag{6}$$

with Fermi potential

$$\mathrm{Im}V_{ij}^F = -\frac{A\hbar}{2}\delta(\vec{r}_{ij}), \qquad A = \left(\frac{2}{\hbar}\right)\frac{Sr_B}{\pi}.$$

Ψ is the bound-state solution of the many-body Schroedinger equation

$$H\Psi = E\Psi \tag{7}$$

with

$$H = T + V^{confine} + V^{Coulomb} \tag{8}$$

The above general formulation can be applied to (i) D+D reactions in metals, (ii) proton-nucleus transmutations, etc. It could be also applied possibly to (iii) biological transmutations. For each case of (i), (ii) and (iii), an appropriate Hamiltonian is to be chosen for Eqs. (7) and (8). To be realistic to a chosen physical system, H could include many degrees of freedom for electrons, metal lattice structures, etc. However, we may have to choose a simpler model Hamiltonian (Eq. (8)) for which Eq. (7) can be solved approximately.

4.3. Importance and significance of the optical theorem formulation of reaction rates (OTF-RRs)

It is important to note differences between Eq. (5) and Eq. (6). Eq. (5) is for nuclear reactions at positive energies (such as for nuclear scattering experiments using beam of nuclei), while Eq. (6) is for nuclear reactions between two nuclei in a bound state (such as deuterons bound in a metal). In the past, Eq. (5) is inappropriately used to argue that low-energy nuclear reactions in metals are impossible. It should be emphasized that the use of Eq. (6) is more appropriate for low-energy nuclear reactions in metals than the use of Eq. (5).

5. BCSNF Theory - Deuterium
In this section, we describe theoretical analysis of the experimental results involving deuterons as applications of the theory of Boson cluster state nuclear fusion (BCSNF) (Eqs. (6), (7), and (8)). This case is applicable for the theoretical explanation of the Fleischmann-Pons effect [2,3] and the deuterium-metals experiments [3-5].

5.1. Boson cluster state (BCS) and BCSNF theory

The Boson cluster states (BCS) include also a possibility of Bose-Einstein condensate (BEC) state. When Boson clusters are non-interacting or weakly interacting, they can form Bose-Einstein condensate (BEC) state which is known to occur at cryogenic temperatures. If Boson clusters have interactions between them, they can form a BCS in a trap at temperatures higher than room temperatures. For a BCSNF to occur, the life time of the BCS needs to be larger than the reaction time (inverse of the reaction rate for DD pair).

For applying the concept of the BCS mechanism to deuteron fusion, we consider N identical charged Bose nuclei (deuterons) confined in a trap (a metal grain/particle or a magnetic trap). For simplicity, we assume an isotropic harmonic potential for the trap to obtain order of magnitude estimates of fusion reaction rates. N-body Schroedinger equation Eq. (7) is solved with the Hamiltonian H for the system given by

$$H = \frac{\hbar^2}{2m}\sum_{i=1}^{N}\Delta_i + \frac{1}{2}m\omega^2\sum_{i=1}^{N}r_i^2 + \sum_{i<j}\frac{e^2}{|\mathbf{r}_i - \mathbf{r}_j|} \tag{9}$$

where m is the rest mass of the Bose nucleus.

The approximate Boson cluster state (BCS) solution of Eq. (7) with H given by Eq. (9) was obtained using the equivalent linear two-body method [11-15].

Using the results of the optical theorem formulation of low energy nuclear reactions [10-12], the ground-state solution was used in Eq. (6) to derive the approximate theoretical formula for the deuteron-deuteron fusion rate in a trap

(magnetic trapping potential or micro/nano-scale metal grain/particle).   The detailed derivations are given elsewhere in references [10 -22].

The use of an alternative method [12] based on the Hartree-Fock mean field theory for bosons [23] yields the same result which is a factor of 2 larger (see Appendix in [12]). This method [12] involves solving a non-linear Schrodinger equation known as the Ginzburg-Pitaevskii-Gross equation [23]. Recent theoretical analysis [24], which includes two-particle correlations, indicates that these additional two-particle correlations cannot alter the results of [12] significantly.

5 2. Reaction rates forthe primary reaction channel

Our final theoretical formula for the total fusion rate R_t for large N case is given by [11,12]

$$R_t = \frac{1}{2\pi}\left(\frac{3}{\pi}\right)^{1/2} S\Omega V n_D^2 \left(\frac{\hbar}{e^2\mu}\right) \tag{10}$$

where μ is the reduced mass, S is the S-factor for the nuclear fusion reaction between two deuterons, n_D is the deuteron number density, and V is the total volume. For D(d,p)T and D(d,n)^{3}He reactions, we have S ≈ 55 keV-barn. We expect also S≈ 55 keV-barn or larger for reaction {1} described below in sub-section 5.3. Only two unknown parameters are (i) the probability of the Boson cluster state(BCS) occupation, Ω, and (ii) the S-factor. Eq. (10) shows that the total fusion rates, R_t, are maximized when $\Omega \approx 1$.

Eq.(10) was derived analytically (no numerical calculations were involved). Eq. (10) provides an important result that nuclear fusion rates R_t for large N case do not depend on the Gamow factor in contrast to the conventional theory for two-body nuclear fusion in free space. There is a simple classical analogy of the Coulomb field suppression. For a uniform spherical charge distribution, the Coulomb field diminishes toward the center and vanishes at the center.

5.3. Reaction mechanism for BCSNF - "Bosenova"

For a single trap containing a large number N of deuterons, the deuteron-deuteron fusion can proceed with the BCSNF.

For the large N case, the deuteron-deuteron reaction   in a Boson cluster state (BCS) can proceed via the following reaction {1}:

{1} $\Psi_{BCS}\{(D+D)+(N-2)D's\} \rightarrow$

$\Psi_{BCS}^*\{^4He+(N-2)D's\}(Q=23.84MeV)$

where the Q-value of 23.84 MeV is shared by ^{4}He and all D's in a BCS, thus maintaining the total momentum conservation in the final state. This implies that the deuteron BCS undergoes a nano-scale explosion due to the total momentum conservation.

This phenomenon/mechanism of nano-explosions of BCS was proposed in 2009 [17]. It is related to a BEC explosion phenomenon occurring with the atomic BEC now known as "Bosenova" [29-31].

For a micro/nano-scale trap of 10 nm diameter containing ~ 3.6 x 10^4 deuterons, each deuteron or ^{4}He will gain only ~ 0.7 keV kinetic energy, if the excess kinetic energy of 23.84 MeV is shared equally. This mechanism of "Bosenova" can provide an explanation for constraints imposed on the secondary reactions by energetic ^{4}He, as described by Hagelstein [32].

Furthermore, as these deuterons slow down in the host metal, they can release electrons from the host metal atoms, thus providing extra conduction electrons which may reduce the resistivity of the host metal.

5.4. Reaction rates for the secondary reaction channels

Other exit channels, D(d,p)T and D(d,n)^{3}He, are expected to have much lower probabilities than that of the exit channel {1}, since both D(d,p)T and D(d,n)^{3}Heinvolve centrifugal and Coulomb barrier transmissions of exit particles in the exit channels, while {1} does not. Thus this mechanism can provide a theoretical explanation for the experimental observation of dominance of the reaction {1} over D(d,p)T and D(d,n)^{3}He in the exit channels.

6.   BCSNF Theory - Hydrogen

In this section, we present a generalization of the theoretical results for one species of Bose nuclei   (deuterons) described in the previous section to the case of two species of Bose nuclei, such as hydrogen-Ni systems investigated by Piantelli et al. [6-8], Rossi et. al. [9], Hadjichristos, et al. [1]. In this section 6 and the next section 7, we limit our theoretical descriptions to the results obtained by Defkalion team, Hadjichristos et al., as described in [1] and in sections 2 and 3.

6.1. Theory

Generalization of The BCSNF theory to the case of two species of Bosons was carried out in 2006 [33].

The reaction rates is given by

$$R_t = \frac{1}{2\pi}\left(\frac{3}{\pi}\right)^{1/2} S_{ij}\sqrt{\Omega_i\Omega_j} V \frac{n_i n_j}{Z_i Z_j}\left(\frac{\hbar}{e^2\mu}\right) \tag{11}$$

where μ is the reduced mass, $\mu = m_i m_j/(m_i + m_j)$.

6.2. One-particle exit reaction channel

As in the case of BCSNF theory for the single specie (deuterium) case of the Fleischmann-Pons effect, the primary reaction channel for this case of hydrogen-metal systems involves one-particle exit reaction channel, which can be written as

$$p + {}^{A}_{Z}X \rightarrow {}^{A+1}_{Z+1}L + Q \tag{12}$$

This one-particle primary reaction channel involves nano-explosion ("Bosenova").

6.3. Two-particles exit reaction channel

For the two-particles exit reactions, examples are,

$$p + {}^{A}_{Z}X \rightarrow {}^{4}He + {}^{A-3}_{Z-1}M + Q \tag{13}$$

Two-particles exit reaction channel producing two nuclei is expected to have the reaction rates which are much slower than that of the one-particle exit reaction channel, as described in sub-section 5.4.

6.4. Multi-particles exit reaction channels

Multi-particles exit reaction channels involving three or more nuclei are expected to have the reaction rates which are much slower than that of the two-particle secondary reaction channel.

7. Reaction Mechanisms for Hydrogen BCSNF

7.1. Triggering mechanisms and magnetic Fields

As described in sub-section 2.2, the heat generating reactions are initiated by plasma ignition method involving the plasma discharge of pressurized hydrogen gas (1-8 bars) in a reaction chamber. An electric power supply was used to provide DC currents of 60-110 mA at 10-24 kV with frequency of ~ kHz between two electrodes which are a pair of spark plugs with specially shaped tungsten and TZM electrodes.

The gas discharge ignition is expected to ionize hydrogen molecules (i) to excited molecular states (including Rydberg molecules), (ii) to excited atomic hydrogen states (including Rydberg atoms), and (iii) protons and electrons (complete dissociation of the hydrogen molecules). During the gas discharges, protons (and other positively charged ions) will be moving toward the cathode, while electrons (and other negatively charged ions) will be moving toward the anode. These moving charges are expected to produce magnetic fields.

7.2. Creations of localized magnetic traps (LMT)

During the triggering stages, moving positive and negative charges are created and are expected to propagate through the reaction cells of ~200 µm sizes inside the Ni foams. The reaction cells contain Ni powders of ~ 5µm sizes. Both Ni foams and powders are no longer magnetic at temperatures above the Curie temperature (~358 ^{0}C or ~631^{0}K) due to heating of the reactor by the plasma gas discharges. However, these moving charges carrying the magnetic fields are expected to induce magnetic field domains in the Ni foams and Ni powders above the Curie temperature, as predicted by Durach, et al. [27]. The above scenario may provide a theoretical explanation of the observe magnetic field of ~ 0.6 Tesla during the triggering period.

These induced magnetic domains are expected to create many localized magnetic fields, randomly distributed on Ni surfaces, which can be regarded as localized magnetic traps (LMT) for hydrogen pairs and molecules. The sizes of LMTs may range from nano-scale to micro-scale.

7.3. Nano-explosion ("Bosenova") and supper current

Hydrogen atoms in the ground state, excited states and/or Rydberg states may interact with each other via electric dipole or magnetic dipole interactions and/or other attractive interactions [34] to form pairs of hydrogen atoms in integer-spin states. These hydrogen pairs or hydrogen molecules may be trapped in an LMT and form a Boson cluster state (BCS) in the LMT. Once the BCS is formed in a LMT, the BCSNF theory described in the previous section 6 can be applied to describe the BCSNF process involving hydrogen.

The reaction rates for this hydrogen-metal system can be estimated using Eq. (13). For the one-particle exit reaction channel described by Eq. (14), the nano-explosion ("Bosenova") mechanism is applicable, producing the excess heat as observed in the experiment described in sub-section 3.1. Furthermore, there will be creation of "supper current" of protons due to the moving proton charges created from many nano-explosions. A substantial fraction of them is directed upward in reaction cells, thus generating the predicted proton super currents.

7.4. Supper current and super magnetic field

These predicted super currents in turn will create super magnetic field which was observed as described in sub-section 3.3. In fact, this mechanism can explain the observed time-correlation between (1) the excess heat generation and (2) the observed generation of super magnetic field of ~1.6 Tesla as described in sub-section 3.3. Therefore this

time correlation can be explained by thenano-explosion mechanism as described above. This in turn supports the nano-explosion ("Bosenova") mechanism for the BCSNF.

The experimental observation of the super magnetic field could serve as a signature of the BCSNF process for future low-energy reaction experiments.

This time correlation may also provide an important possibility that direct partial conversion of excess power generation to electric power may be possible utilizing the super magnetic field.

7.5 Self-sustainability

If the reaction rates can be made to be sufficiently large for the above reaction mechanism/scenario, the interval between two successive triggering can be made longer, leading to self-sustaining the BCSNF.

7.6. Roles of Ni isotopes and even-isotope effect

As described in section 3, there were no gamma rays observed with energy range outside of 50keV – 300keV. Therefore, we can rule out hydrogen-Ni fusion reactions described by Eq. (12), since emissions of hard gamma rays are expected from the process described by Eq.(12).
However, as discussed in the previous sub-section, Ni metal and its magnetic properties play very important roles in creating the LMTs which facilitates BCSNF of hydrogen and creating nano-explosion ("Bosenova") which produces the excess heat and magnetic fields.

Furthermore, the above BCSNF mechanism also explains the even-isotope effect that the excess heat was observed only with the even isotopes of Ni, as described in sub-section 3.4. This is consistent with the prediction made in 2006 [33] that Bosons (the hydrogen-pair clusters) cannot coexist with fermions (odd isotopes of Ni) in the same LMT [33].

7.7. Roles of deuteron and other light nuclei impurities

Since hydrogen-Ni may not involved as primary fusion reactions as described in the previous section VI.F, there are possibilities that other light nuclei present as impurities may be participating in the BCSNF processes. One example is the primary reaction described by Eq. (14) involving deuteron impurity (1.25×10^{-4}%):

$$p + d \rightarrow {}^3He + 5.494 MeV \tag{14}$$

We note that, in 2002, Swartz et al. observed excess heat production from electrolysis experiments with the ordinary water plus the heavy water using Ni cathode [35].

For experiments with Defkalion's Hyperion reactor, we need to investigate the effect of the primary reaction, Eq. (14), for excess heat production by increasing the deuterium density.

8.   Summary and Future Prospects

Defkalion's Hyperion R-5 reactor has been demonstrated to be a reliable working device producing excess heat at sufficiently high level with reliable control and high reproducibility for further scientific investigations and for practical applications. The experimental results obtained with the HyperionR-5 reactor are described in some details.

For theoretical analysis of the experimental data generated by the Hyperion R-5 reactor, the theory of the Boson cluster state nuclear fusion (BCSNF) is used. The BCSNF is a generalization of the optical theorem formulation to low energy nuclear reactions occurring in deuterium/hydrogen loaded metal systems.

It is shown that the BCSNF theory is capable of explaining qualitatively or quantitatively most of the experimental results and observations reported from experiments with the Hyperion R-5 reactor. In particular, the observed time-correlation between the super magnetic field and the excess heat generations can be explained by the BCSNF theory involving nano-explosions ("Bosenova"), which create the super current and the super magnetic field as well as the excess power generation. The observed super magnetic field is a new phenomenon and a new scientific discovery. It opens up a possibility of direct conversion of excess heat generation to electric power utilizing the super magnetic field.

Defkalion has recently acquired new two on-line real-time mass spectrometers [27] which will be integrated with Hyperion R-6 reactors.   These integrated experimental systems are expected to generate the experimental data for the reaction products which are urgently needed for theoretical and scientific understanding of nuclear-reaction dynamics in this emerging field.

So far, the theoretical reaction-rate formulae, (Eq. (11), etc.) were based on analytical solutions of the approximate time-independent Schrödinger equations for many-body systems using the Hartree-Fock theory with correlation effects. This corresponds to time-independent non-liner (TINL) dynamics. Such analytical formulae for reaction rates are extremely useful for initial qualitative analysis of the experimental data.   For more quantitative analysis of experimental data, we will need the time-dependent non-linear Schrödinger equations for many-body systems (time-dependent non-linear (TDNL) dynamics).

Experimental works described in sections 2 and 3 were carried out by John Hadjichristos (JH) and his team members at Defkalion, while the theoretical development and analysis described in sections 4 – 7 were carried out by Yeong E. Kim (YEK). We thank all members of the Defkalion team for their efforts for the experimental work and for their inputs for this manuscript. Sections 2 and 3 were written by JH while sections 4 – 7 were written by YEK. The entire manuscript was co-edited by both JH and YEK.

References

[1] J. Hajichristos, M. Koulouis, and A. Chatzichristos, "Technical characteristics and performance of the Defkalion's pre-industrial product," to be published in the proceeding of the ICCF-17, Daejeon, Korea 2012.

[2] M. Fleischman and S. Pons, "Electrochemically Induced Nuclear Fusion of Deuterium," J. Electroanal. Chem. **261**, 301 (1989); Errata, J. Electroanal. Chem. **263**, 187 (1989).

[3] P.L. Hagelstein, et al., "New Physical Effects in Metal Deuterides," Proceedings of ICCF-11, Marseille, France, *Condensed Matter Nuclear Science,* pp. 23-59, World Scientific Publishing Co., Singapore (2006) and references therein.

[4] Y. Arata and Y.C. Zhang, J. High Temp. Soc**34** (2), 85 (2008).

[5] A. Kitamura, et al., Phys. Lett. A**373**, 3109 (2009), and references

[6] E. G. Campari, S. Focardi, V. Gabbani, V. Montalbano, F. Piantelli, S. Veronesi, Atti*TESMI Workshop*, Lecce, december 6-7 2002, A. Lorusso and V. Nassisi, editors, 35-42 (2004).

[7] S. Focardi and F. Piantelli, "Anomalous effect between 200 and 400 C on Ni-H systems, Neither chemical nor electrochemical phenomenon" in "*COLD FUSION: the history of research in Italy*", published by ENEA, Italian Agency for Technologies, Energy and Environment (2009), pp. 171-182, and references therein.

[8] Francisco Piantelli, "METHOD FOR PRODUCING ENERGY AND APPARATUS THEREFOR," International Patent Application Publication (Int. Pub. No. : WO 2010/058288 A1, Pub. Date: May 27, 2010.

[9] Andrea Rossi, "METHOD AND APPARATUS FOR CARRYING OUT NICKEL AND HYDROGEN EXOTHERMAL REACTION," United States Patent Application Publication (Pub. No.: US 2011/0005506 A1, Pub. Date: Jan.13, 2011).

[10] Y. E. Kim, Y. J. Kim, A. L. Zubarev and J. H. Yoon, "Optical Theorem Formulation of Low-Energy Nuclear Reactions," Phys. Rev. C **55**, 801 (1997).

[11] Y. E. Kim and A. L. Zubarev, "Nuclear Fusion for Bose Nuclei Confined in Ion Traps," Fusion Technology **37**, 151(2000).

[12] Y. E. Kim and A. L. Zubarev, "Ultra low-energy nuclear fusion of Bose nuclei in nano-scale ion traps," Italian Physical Society Proceedings **70**, 375 (2000).

[13] Y. E. Kim and A. L. Zubarev, "Equivalent linear two-body method for many-body problems," Phys. B: At. Mol. Opt. Phys. **33**, 55-69 (2000).

[14] Y. E. Kim and A. L. Zubarev, "Ground state of charged bosons confined in a harmonic trap," Phys. Rev. A **64**, 013603-1 (2001).

[15] Y. E. Kim and A. L. Zubarev, "Equivalent linear two-body method for Bose-Einstein condensates in time-dependent harmonic traps," Phys. Rev. A**66**, 053602-1 (2002).

[16] Y. E. Kim and A. L. Zubarev, "Time-dependent density-functional theory for trapped strongly interacting fermionic atoms," Physical Review A**70**, 033612 (2002).

[17] Y. E. Kim, "Theory of Bose-Einstein Condensation Mechanism for Deuteron-Induced Nuclear Reactions in Micro/Nano-Scale Metal Grains and Particles,"Naturwissenschaften **96**, 803 (2009) and references therein.

[18] Y. E. Kim, "Bose-Einstein Condensate Theory of Deuteron Fusion in Metal," J. Condensed Matter Nucl. Sci. **4**, 188 (2010), Proceedings of Symposium on New Energy Technologies, the 239th National Meeting of American Chemical Society, San Francisco, March 21-26, 2010.

[19] Y. E. Kim, "Theoretical interpretation of anomalous tritium and neutron productions during Pd/D co-deposition experiments," Eur. Phys. J. Appl. Phys. **52**, 31101 (2010).

[20] Y. E. Kim, "Nuclear Reactions in Micro/Nano-Scale Metal Particles," Few-Body Systems **54**, 25-30 (2013). Invited paper presented at the 5th Asia-Pacific Conference on Few-Body Problems in Physics (APFB2011), Seoul, Korea, August 22-26, 2011.

[21] Y. E. Kim, "Cryogenic Ignition of Deuteron Fusion in Micro/Nano-Scale Metal Particles," Purdue Nuclear and Many Body Theory Group (PNMBTG) Preprint PNMBTG-11-2011 (November 2011). Invited paper presented at Topical Meeting of the 2012 Nuclear and Emerging Technologies for Space (NETS), the 43rd Lunar and Planetary Science Conference, March 19-23, 2012, the Woodlands, Texas.

[22] Y. E. Kim, "Conventional nuclear theory of low energy nuclear reactions in metals: alternative approach to clean nuclear fusion energy generation," J. Condensed Matter Nucl. Sci. **12**, 1-13 (2012), invited talk presented at the ICCF-17, Daejeon, Korea, 2012.

[23] B. D. Esry, "Hartree-Fock theory for Bose-Einstein condensates and the inclusion of correlation effects," Phys. Rev. A**55**, 1147 (1997).

[24] Y. E. Kim, "Hartree-Fock Theory with Correlation Effects Applied to Nuclear Reaction Rates for Charged Bose Nuclei Confined in a Harmonic Trap," Purdue Nuclear and Many Body Theory Group (PNMBTG) Preprint PNMBTG-8-2013 (August, 2013).

[25] "Test Protocol for Public Demonstrations of the Hyperion R5", http://18.resaerch.missouri.edu/Protocol_and_test_results.pdf

[26] K. Ostrikov, E. C. Neyts, and M. Meyyappan, "Plasma Nanoscience: from Nano-Solids in Plasmas to Nano-Plasmas in Solids," Advances in Physics **62**, 113-224 (2013). DOI: 10.1080/0001872.2013.808047http://arxiv.org/abs/1306.6711

[27] M. Durach, A. Rusina, and M. Stockman, "Giant Surface-Plasmon-Induced Drag Effect", Photonic Metamaterials and Plasmonics. Tucson, Arizona US, June 7-8, 2010. Plasmonics IV (MTuC), http://dx.doi.org/10.1364/PMETA_PLAS.2010.MTuC5

[28] D. Papanastasiou, I. Orfanopoulos, D. Kounadis, A. Lekkas, I. Nikolos, R. Giles, A. Entwistle, E. Raptakis, "Performance Characterization of a Differential Mobility Spectrometer Operated in Laminarized Low Pressure Subsonic Flows," IMS Workshop, ASMS Annual Conference 2013.

[29] J. L. Roberts, et al., "Controlled collapse of a Bose-Einstein Condensate," Phys. Rev. Lett. **86**, 4211(2001).

[30] E. A. Donley, et al., "Dynamics of collapsing and exploding Bose-Einstein condensates," Nature **412**, 209 (July 2001).

[31] M. H.P.M. van Putten, "Pair condensates produced in bosenovae," Phys. Lett. A **374**, 3346(2010).

[32] P. L. Hagelstein, Naturwissenschaften **97**, 345(2010).

[33] Y. E. Kim and A. L. Zubarev, "Mixtures of charged bosons confined in harmonic traps and Bose-Einstein condensation mechanism for low-energy nuclear reactions and transmutation processes in condense matters," in the proceedings of the ICCF-11, Marseilles, France, 2006, pp. 711-717.

[34] P. K. Shukla and B.Eliasson, "Novel Attractive Force between Ions in Quantum Plasmas," Phys.Rev. Lett. 108, 165007 (2012).

[35] M. R. Swartz, G. M. Verner, and A. H. Frank, "The impact of heavy water (D$_2$O) in Nickel-light water cold fusion systems," in the ICCF-9 Proceedings, *Condensed Matter Nuclear Science*, pp. 335-342 (2003).